Supporting Information for

Vapochromic behaviour of a nickel(II)-quinonoid complex with dimensional changes between 1D and higher

Ryota Yano,[a] Masaki Yoshida,*[a] Takahiro Tsunenari,[a] Ayana Sato-Tomita,[b] Shunsuke Nozawa,[c] Youhei Iida,[d] Noriaki Matsunaga,[d] Atsushi Kobayashi,[a] and Masako Kato*[a]

[a] Department of Chemistry, Faculty of Science, Hokkaido University, North-10 West-8, Kita-ku, Sapporo, Hokkaido 060-0810, Japan.

[b] Division of Biophysics, Department of Physiology, Jichi Medical University, 3311-1 Yakushiji, Shimotsuke, Tochigi 329-0498, Japan.

[c] Institute of Materials Structure Science, High Energy Accelerator Research Organization (KEK), 1-1 Oho, Tsukuba, Ibaraki 305-0801, Japan.

[d] Department of Physics, Faculty of Science, Hokkaido University, North-10 West-8, Kita-ku, Sapporo, Hokkaido 060-0810, Japan.

E-mail: myoshida@sci.hokudai.ac.jp, mkato@sci.hokudai.ac.jp

Table of Contents

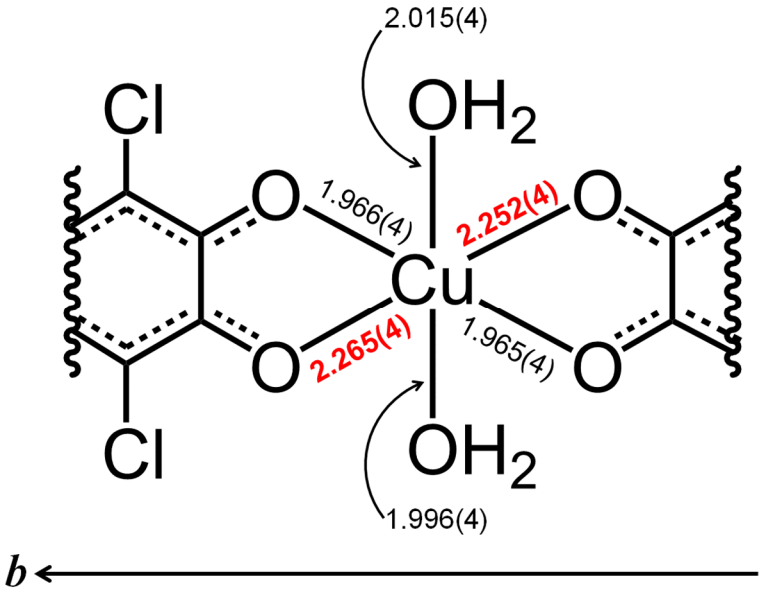

Scheme S1 Cu-O bond distances (Å) of $\{Cu(ca)(OH_2)_2\}_n \cdot nH_2O$,[S1] showing clear Jahn-Teller distortion. Because such Jahn-Teller distortion is absent in **2-H₂O**, the *b* axis of **2-H₂O** is shortened compared to that of $\{Cu(ca)(OH_2)_2\}_n \cdot nH_2O$.

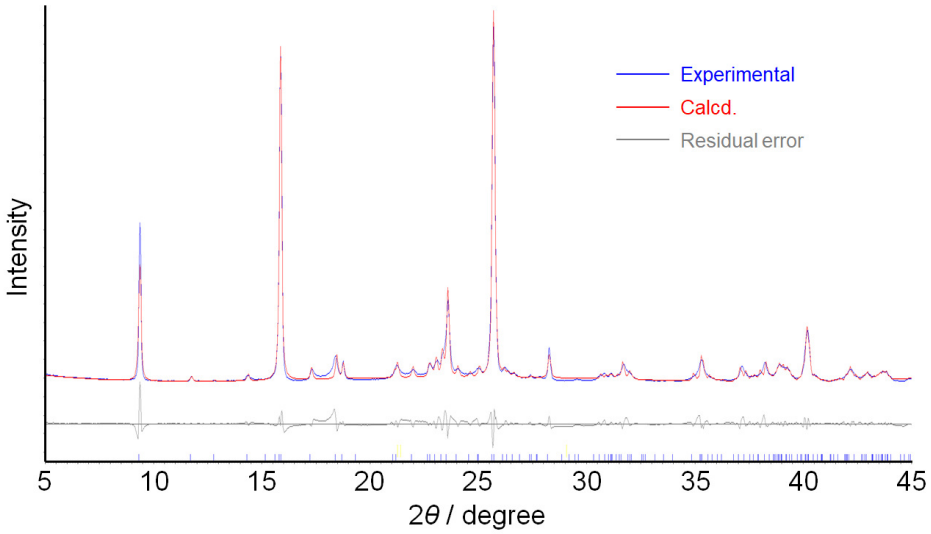

Fig. S1 Experimental PXRD pattern of **2-H₂O** (blue line; taken from the data given in Fig. 1), and calculated PXRD pattern by optimising the crystal parameters of $\{Cu(ca)(OH_2)_2\}_n \cdot nH_2O$ (red line). Gray line indicates the difference between the experimental and calculated PXRD patterns. Short blue vertical bars below the difference pattern indicate the positions of allowed Bragg reflections.

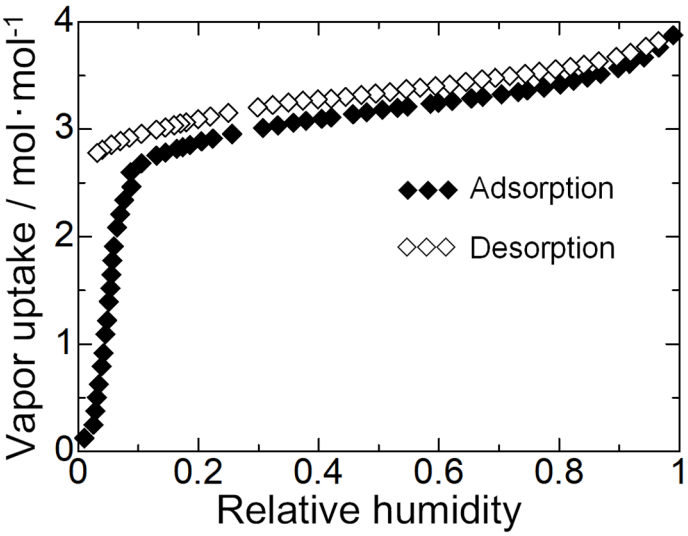

Fig. S2 Water-vapour adsorption isotherm of **2** at 298 K. Closed and open symbols indicate adsorption and desorption, respectively.

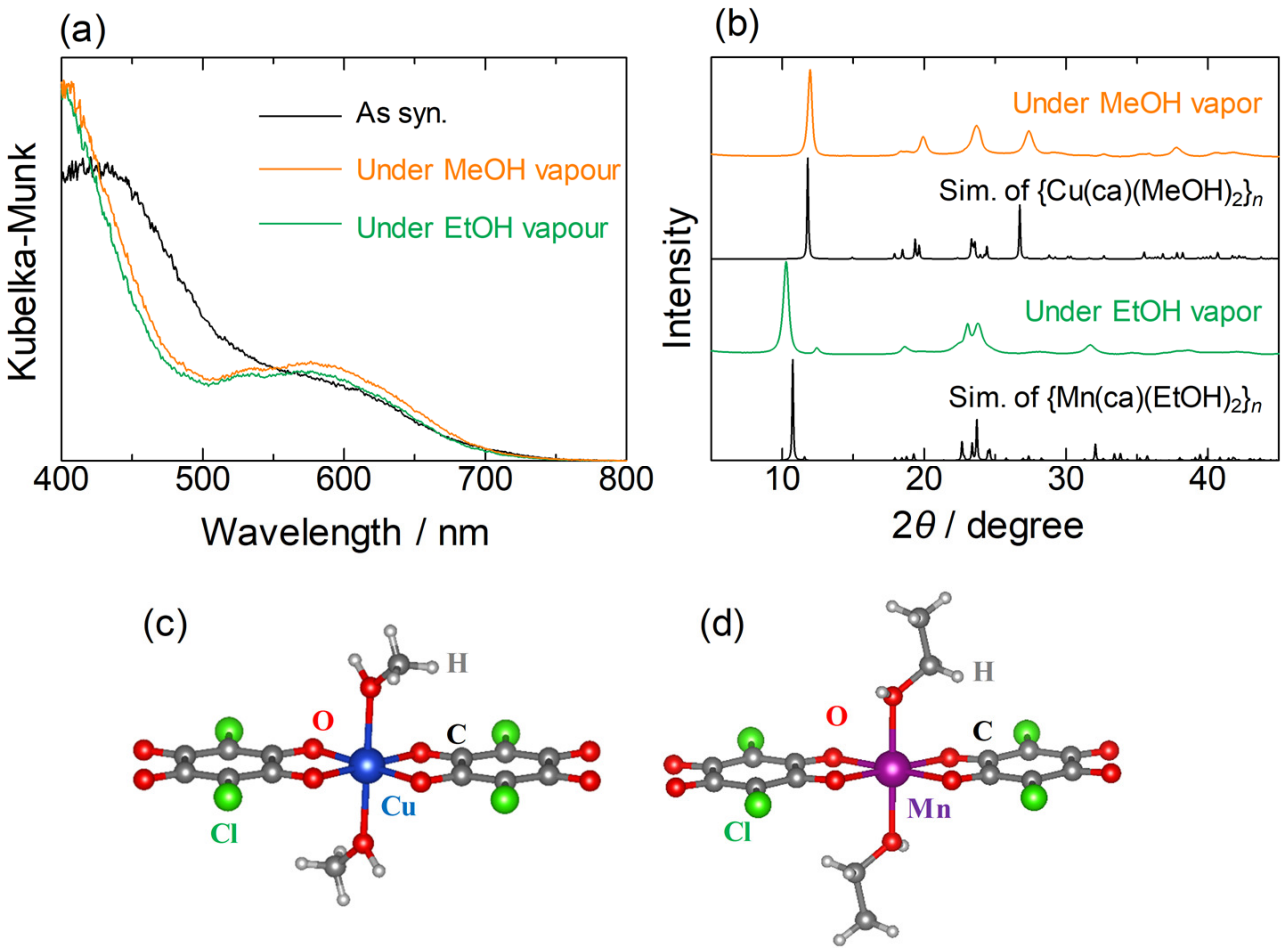

Fig. S3 (a) Changes of the diffuse reflectance spectrum of **2-H$_2$O** (As syn.) by heating and the exposure to the MeOH (orange line) or EtOH (green line) vapour. (b) PXRD patterns of dried **2** after the exposure to the MeOH vapour (green line) and the EtOH vapour (orange line). Black lines indicate the simulated patterns calculated from the crystal structures of previously reported complexes $\{Cu(ca)(MeOH)_2\}_n$[S2] and $\{Mn(ca)(EtOH)_2\}_n$.[S3] (c,d) Crystal structures around the coordination spheres of (c) $\{Cu(ca)(MeOH)_2\}_n$ and (d) $\{Mn(ca)(EtOH)_2\}_n$.

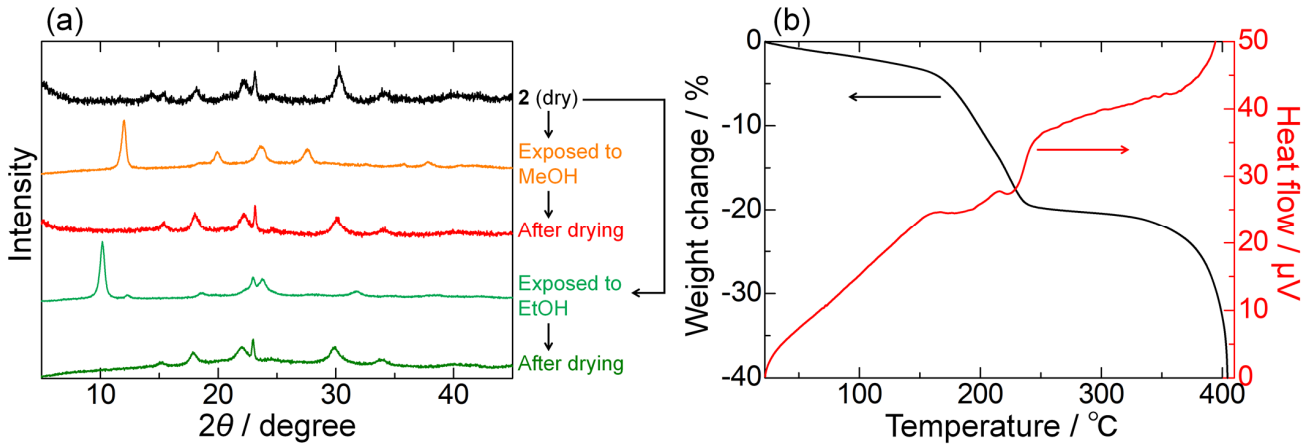

Fig. S4 (a) Changes of the PXRD patterns of **2** during vapour exposure-drying processes, showing the reversibility of the vapochromism. (b) Thermogravimetric analysis and differential thermal analysis of **2** after MeOH vapour exposure. A weight loss of 16.5% from 160 to 250 °C is assignable to the release of 2 molecules of methanol from $\{Ni(ca)(MeOH)_2\}_n$ (theoretical value: 19.4%). The DTA curve showed two peaks at 180 and 223 °C, corresponding to the stepwise release of 2 coordinated methanol molecules.

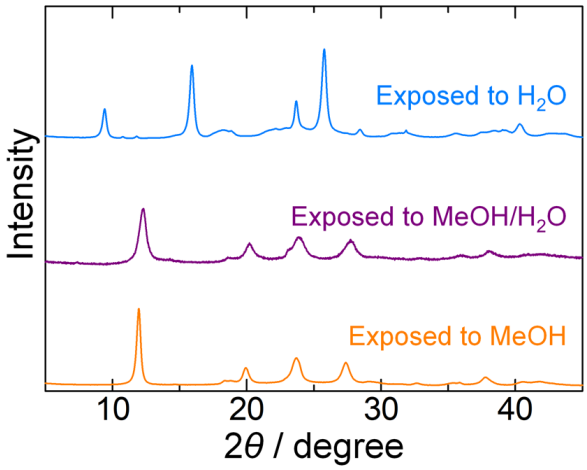

Fig. S5 PXRD pattern of dried **2** after the exposure to the saturated MeOH/H_2O vapour for 50 h at 30 °C using MeOH/H_2O = 1/1 (v/v) mixture (purple line). The PXRD pattern is almost identical to that of the MeOH-exposed form (orange), and quite different from that of the H_2O-exposed form (blue). This difference would be originated from the differences in the saturation vapour pressures (4.2 kPa for water, 22 kPa for methanol, at 30 °C).

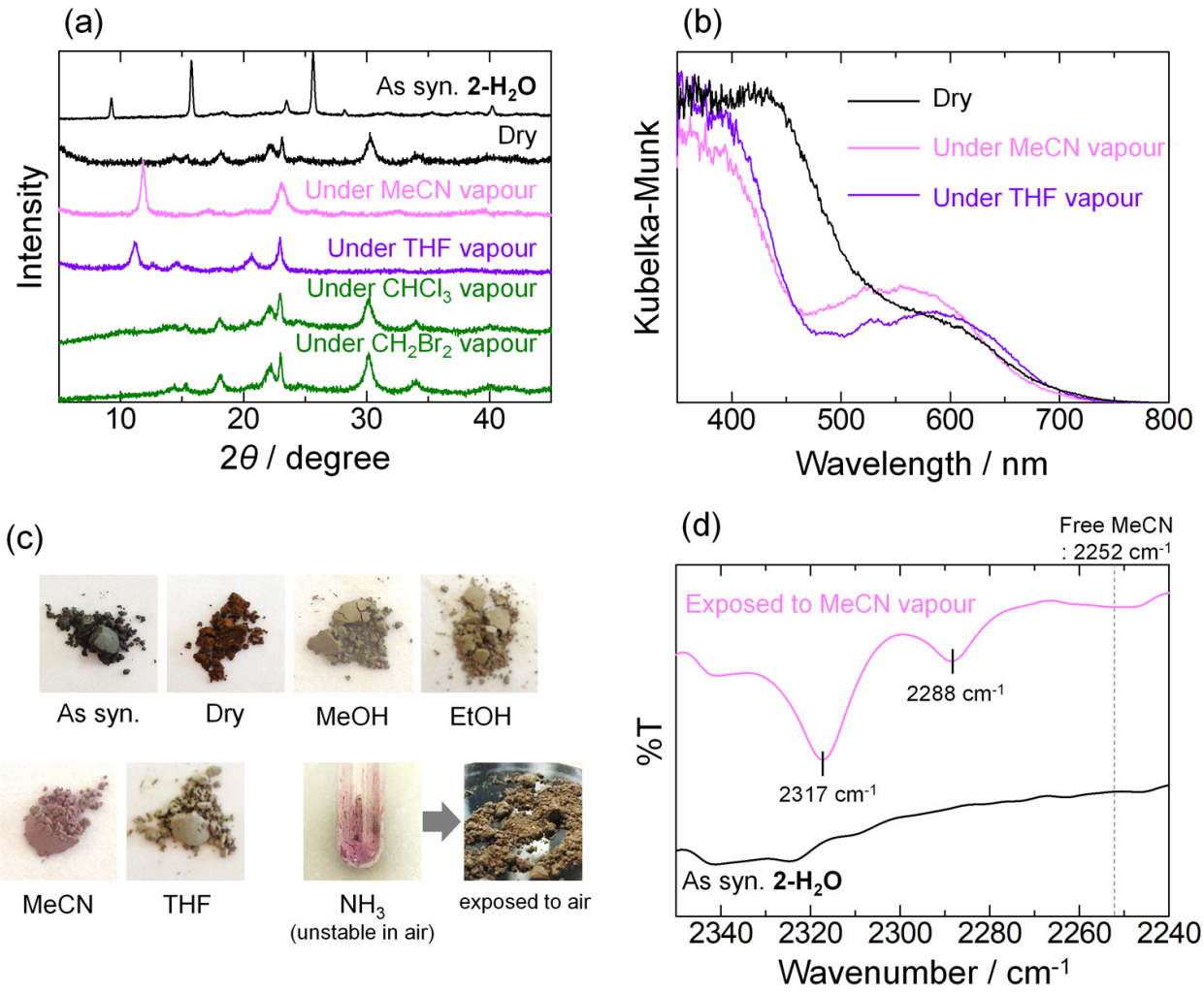

Fig. S6 Changes of (a) the PXRD pattern (b) and the diffuse reflectance spectrum of **2** under several vapours, and (c) photographs of **2** during the vapochromic process. For the NH_3-exposed form, PXRD and diffuse reflectance measurements were difficult because of the instability in air. Although crystal structures after vapour exposure are still unknown, the colour and crystal structure changed after exposure to the coordinating vapours (i.e., alcohols, MeCN, THF, and NH_3). Indeed, the coordination of MeCN was confirmed by (d) the IR spectrum of the MeCN-exposed form showing peaks at 2317 and 2288 cm^{-1}, which were absent in **2-H₂O**. These peaks are attributed to the ν(C≡N) stretching of coordinated MeCN,[S4] and are clearly different from that of free MeCN (2252 cm^{-1}).[S4a]

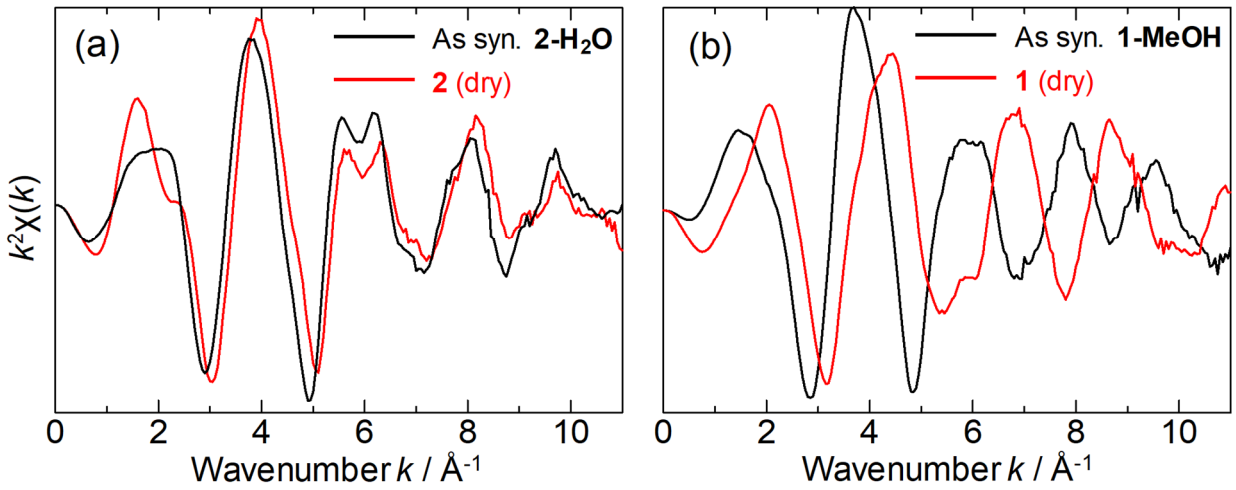

Fig. S7 Changes of the k^2-weighted EXAFS spectra of the Ni-*K* edge of (a) **2-H₂O** and (b) **1-MeOH** before (black lines) and after (red lines) the removal of vapour molecules.

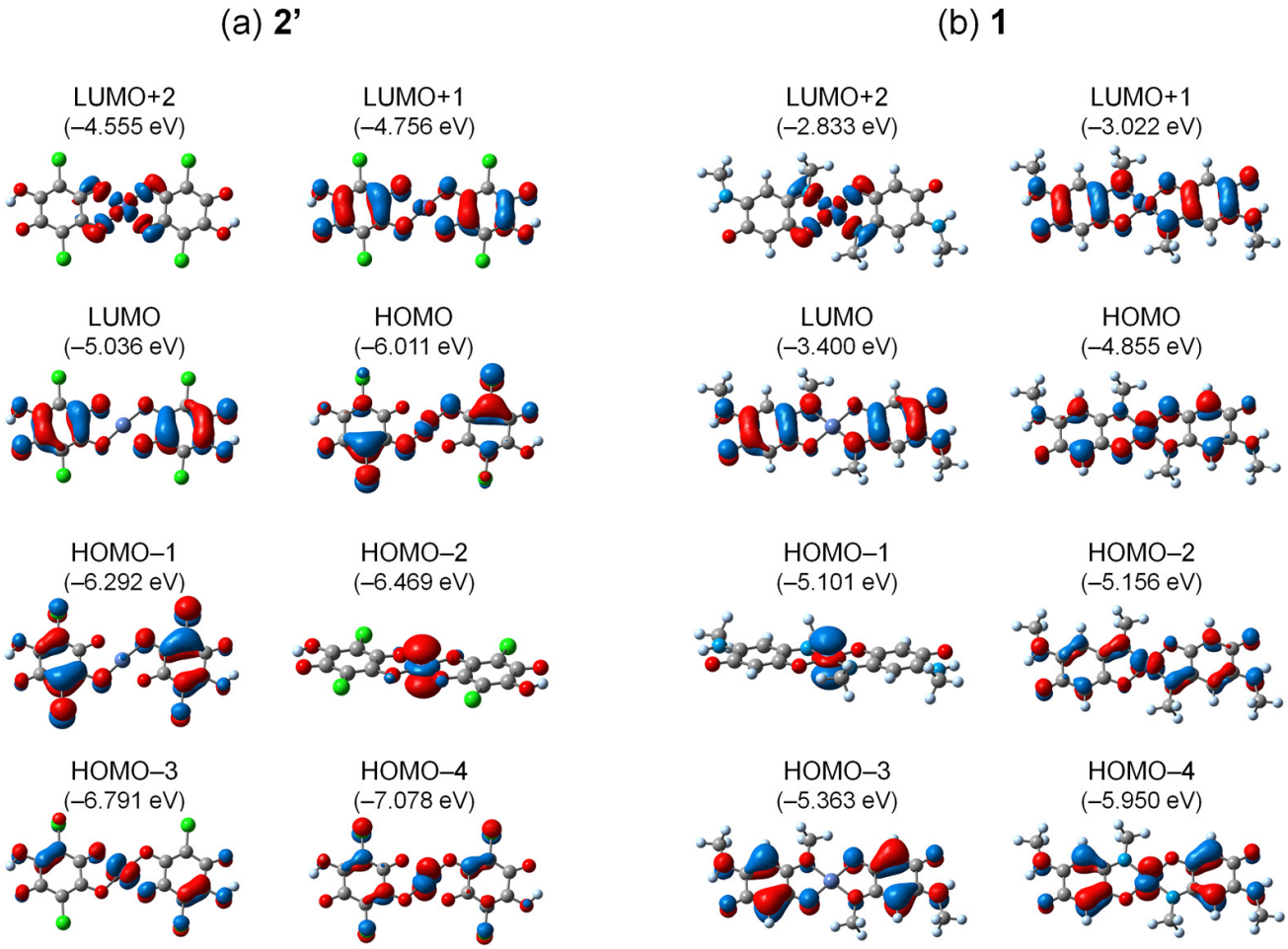

Fig. S8 Kohn-Sham orbitals (isovalue = 0.035) in the frontier region of optimised ground state structures of (a) **2'** (partial structure of **2**) and (b) **1**.

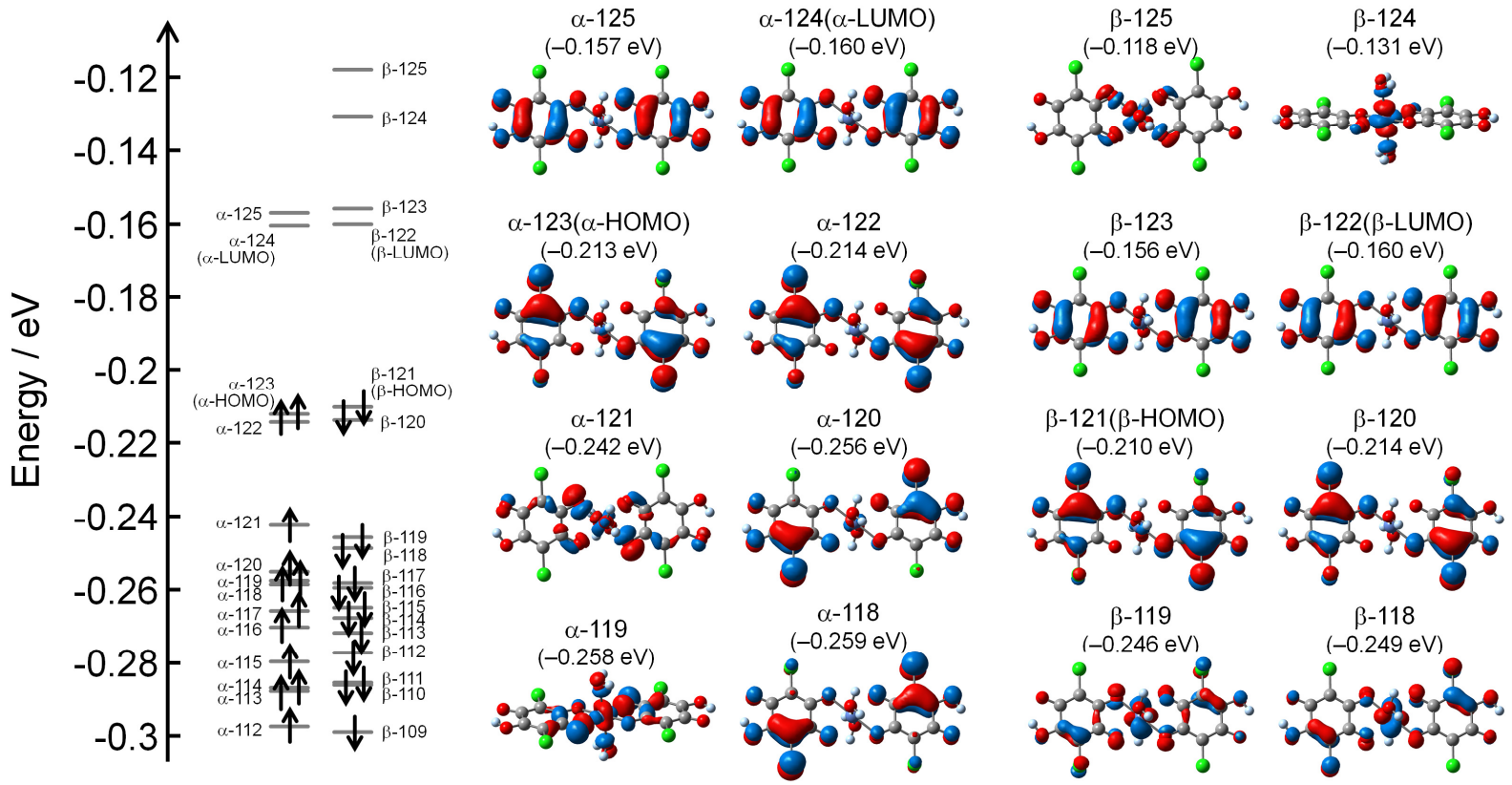

Fig. S9 Selected Kohn-Sham orbitals (isovalue = 0.035) and the energy level diagram in the frontier region of optimised ground state structure of **2'-H_2O** (partial structure of **2-H_2O**).

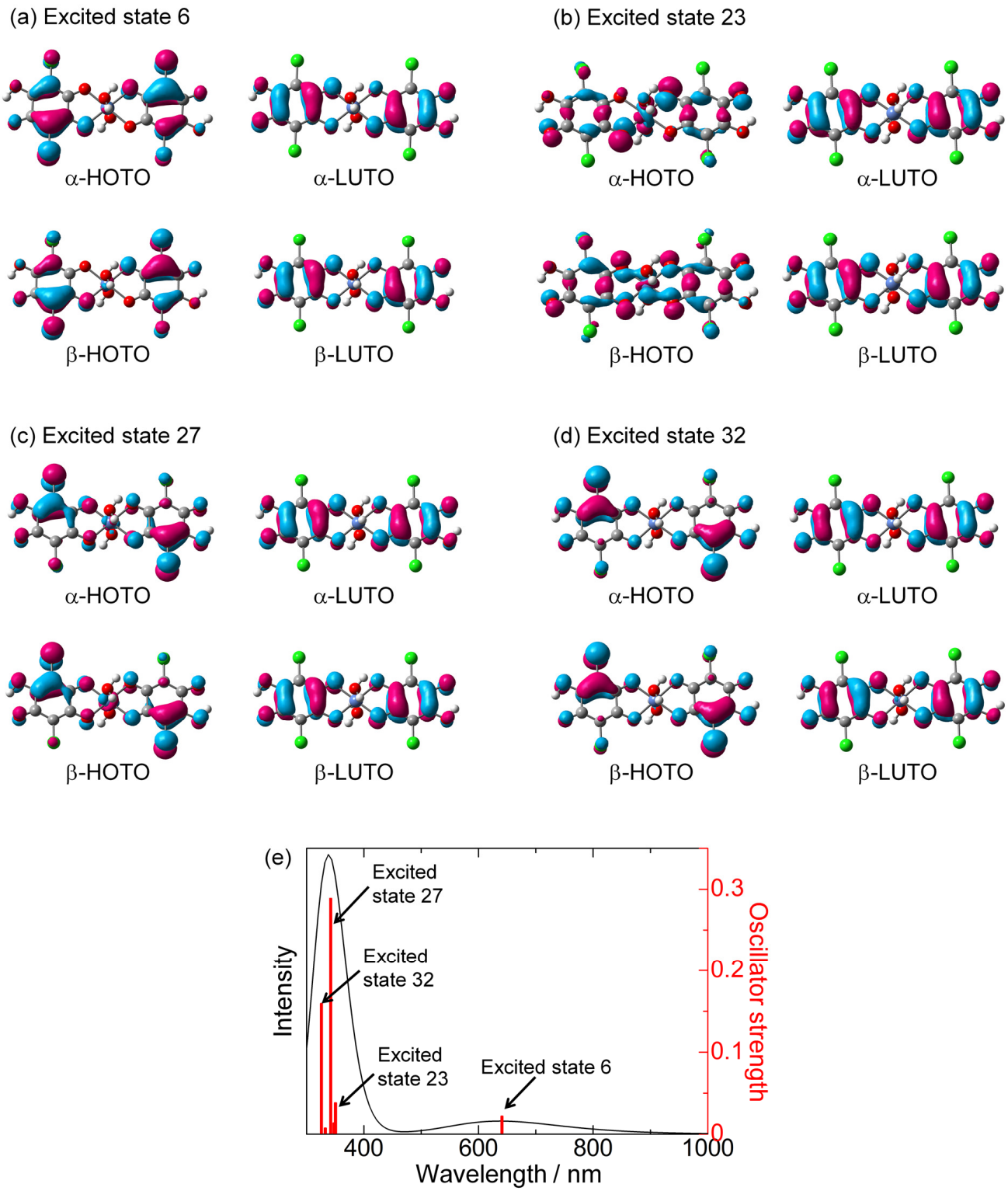

Fig. S10 (a-d) Natural transition orbitals (NTOs) of **2'-H_2O** for the important vertical excitations: (a) 6th (λ_{calcd} = 642 nm, f = 0.0220), (b) 23rd (λ_{calcd} = 349 nm, f = 0.0137), (c) 27th (λ_{calcd} = 343 nm, f = 0.2887), and (d) 32nd (λ_{calcd} = 327 nm, f = 0.1594). HOTO and LUTO denote the highest occupied transition orbital and the lowest unoccupied transition orbital, respectively. (e) Simulated UV-vis absorption spectrum (black line) and the oscillator strengths (red bars) of **2'-H_2O**.

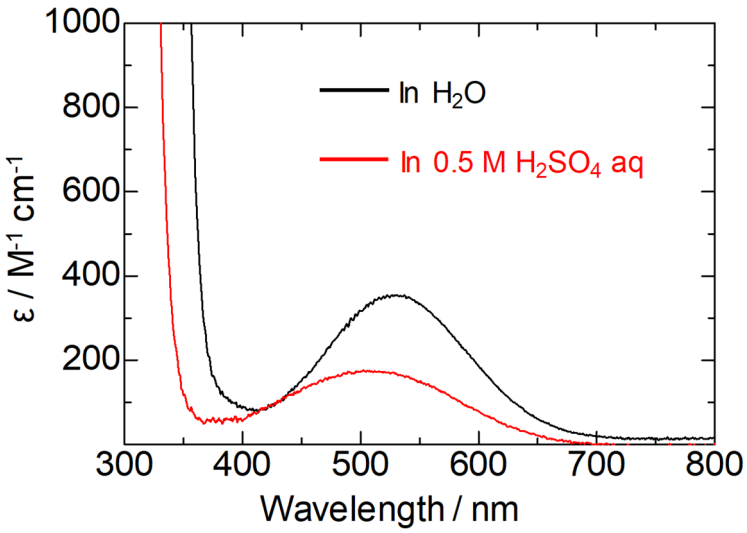

Fig. S11 UV-vis absorption spectrum of H_2ca in water (black line; pH 0.21) and in an aqueous 0.5 M H_2SO_4 solution (red line; pH 2.77). Considering the pK_a values of H_2ca (pK_{a1} = 0.76 and pK_{a2} = 3.08),[S5] H_2ca is fully protonated in an aqueous 0.5 M H_2SO_4 solution, while one of the two protons is removed in water.

Table S1 Cartesian coordinates for the optimised structure of **2'**.

Ni	0.000513	0.01315	0.039573	C	-2.53381	0.710876	0.009089
O	-1.32277	-1.27604	0.022509	C	-3.73845	1.454439	-0.01409
O	-1.38732	1.246846	0.024545	C	-4.92982	-0.78974	-0.01884
O	1.376735	-1.23121	0.021746	O	6.070078	1.250208	-0.04395
O	1.333556	1.291816	0.057154	O	-6.06025	-1.27273	-0.02806
C	2.527655	-0.70469	0.009901	O	6.075262	-1.29536	-0.04839
C	4.935891	0.776487	-0.02282	H	6.69836	-0.52645	-0.05801
C	3.726298	-1.45798	-0.00973	O	-6.08615	1.272752	-0.04557
C	2.518144	0.780615	0.023123	H	-6.70311	0.498867	-0.04812
C	3.700595	1.485815	0.00297	Cl	-3.7056	3.16965	-0.02094
C	4.891943	-0.74604	-0.02514	Cl	-3.68035	-3.2033	0.01005
C	-2.51183	-0.77425	0.009635	Cl	3.706159	3.200145	0.009229
C	-4.89827	0.733069	-0.02792	Cl	3.679735	-3.17286	-0.01581
C	-3.68864	-1.48902	-0.0003				

Table S2 Cartesian coordinates for the optimised structure of **1**.

Ni	0.000000	0.000002	-0.000014	N	1.538502	-1.07868	0.000031
O	-1.207163	-1.420564	0.000099	N	6.328211	-0.42798	-0.000145
O	-5.874001	-2.129612	-0.000153	C	2.672659	-0.40913	0.000024
N	-1.538503	1.078684	-0.000054	C	3.978396	-0.94899	0.000093
N	-6.328211	0.427971	0.000173	C	5.041453	-0.07481	-0.000005
C	-2.672659	0.409134	-0.000034	C	4.852147	1.435072	-0.000002
C	-3.978396	0.948991	-0.000087	C	3.517166	1.924642	-0.000065
C	-5.041451	0.07481	0.00002	C	2.451669	1.056676	-0.000062
C	-4.852145	-1.435071	0.000015	C	1.548635	-2.52531	0.000095
C	-3.517164	-1.92464	0.000063	C	6.79932	-1.78436	0.000228
C	-2.451668	-1.056674	0.000049	H	4.126915	-2.02269	0.000198
C	-1.548636	2.525316	-0.000116	H	6.964388	0.365437	0.000131
C	-6.799326	1.784354	-0.000192	H	3.3582	2.995671	-0.000066
H	-4.126916	2.022686	-0.000189	H	0.522533	-2.88709	-0.000005
H	-6.964383	-0.365448	-0.000089	H	2.062966	-2.91422	-0.886528
H	-3.358199	-2.995669	0.000063	H	6.449691	-2.32593	0.886841
H	-0.522534	2.887096	-0.000034	H	6.447983	-2.32686	-0.885124
H	-2.062949	2.914217	0.886518	H	2.06275	-2.91414	0.886877
H	-6.449706	2.325919	-0.886807	H	-2.06277	2.914145	-0.886886
H	-6.447986	2.326851	0.885158	H	-7.88786	1.792887	0.000878
O	1.207164	1.420566	-0.000127	H	7.887852	-1.7929	-0.000834
O	5.874004	2.129612	0.000195				

Table S3 Cartesian coordinates for the optimised structure of **2'-H_2O**.

Ni	0.000003	0.000148	0.000178	C	-2.66715	-0.78792	0.072984
O	-1.51241	-1.31117	0.133397	C	-5.07357	0.724348	-0.02266
O	-1.58095	1.306736	0.138095	C	-3.86434	-1.48254	0.029306
O	1.580804	-1.30659	-0.13791	C	-2.6869	0.737619	0.076858
O	1.512505	1.311346	-0.13304	C	-3.92125	1.448777	0.032566
O	0.230961	-0.03347	2.124176	C	-5.10243	-0.79564	-0.02555
H	-0.06521	0.799086	2.507905	O	6.235905	1.277323	0.073373
H	-0.3491	-0.71344	2.485186	O	-6.2358	-1.27761	-0.07336
O	-0.2309	0.033694	-2.12382	O	6.266832	-1.25435	0.073426
H	0.349143	0.71366	-2.48484	H	6.863236	-0.46332	0.102209
H	0.065281	-0.79886	-2.50754	O	-6.26693	1.254063	-0.07409
C	2.68683	-0.73756	-0.07721	H	-6.86326	0.462977	-0.10303
C	5.102512	0.795462	0.025167	Cl	-3.91836	3.171337	0.041892
C	3.921113	-1.44884	-0.03297	Cl	-3.86663	-3.20667	0.03668
C	2.667205	0.787983	-0.07287	Cl	3.866898	3.206612	-0.03608
C	3.864468	1.482481	-0.02924	Cl	3.918064	-3.1714	-0.04239
C	5.073511	-0.72452	0.022208				

Table S4 Computed vertical excitations of **2'-H_2O**.

Excited State 1:	4.124-A	1.1140 eV	1112.97 nm	*f*=0.0000	<S**2>=4.002
122A ->125A	0.47653				
123A ->124A	0.52690				
120B ->123B	-0.47040				
121B ->122B	0.53129				
Excited State 2:	4.124-A	1.1172 eV	1109.73 nm	*f*=0.0000	<S**2>=4.001
122A ->124A	0.51304				
123A ->125A	0.49169				
120B ->122B	-0.51182				
121B ->123B	0.49080				
Excited State 3:	3.002-A	1.5100 eV	821.08 nm	*f*=0.0000	<S**2>=2.004
99B ->124B	0.16703				
101B ->124B	-0.19274				
105B ->124B	0.20924				
105B ->125B	0.13475				
108B ->124B	-0.62429				
108B ->125B	0.31280				
108B ->126B	0.13543				
111B ->124B	0.51306				
111B ->126B	-0.16718				
119B ->124B	-0.10871				
119B ->125B	0.10851				
121B ->124B	0.14966				
108B <-124B	-0.11917				
Excited State 4:	3.002-A	1.5552 eV	797.23 nm	*f*=0.0000	<S**2>=2.004
97B ->124B	0.12367				
101B ->124B	0.12781				
105B ->124B	0.43108				
105B ->125B	0.19791				
105B ->126B	-0.16714				
108B ->124B	0.52489				
108B ->126B	-0.14523				
111B ->124B	0.39454				

(Continued)

111B ->125B	0.30009				
111B ->126B	-0.17185				
119B ->124B	0.23306				
121B ->124B	0.19928				
121B ->125B	0.10625				
Excited State 5:	3.002-A	1.7379 eV	713.43 nm	*f*=0.0000	<S**2>=2.003
103B ->125B	-0.31983				
104B ->124B	0.14901				
104B ->125B	-0.56550				
110B ->125B	-0.25284				
113B ->125B	0.19406				
115B ->124B	-0.15887				
115B ->125B	0.58981				
116B ->125B	-0.21334				
Excited State 6:	3.004-A	1.9322 eV	641.69 nm	*f*=0.0220	<S**2>=2.006
122A ->125A	-0.43053				
123A ->124A	-0.55687				
120B ->123B	-0.41456				
121B ->122B	0.57068				
Excited State 7:	3.003-A	1.9430 eV	638.10 nm	*f*=0.0000	<S**2>=2.005
122A ->124A	0.53215				
123A ->125A	0.45866				
120B ->122B	0.53131				
121B ->123B	-0.46121				
Excited State 8:	4.124-A	2.1252 eV	583.41 nm	*f*=0.0000	<S**2>=4.001
120A ->125A	-0.45619				
121A ->124A	-0.50675				
118B ->123B	0.45468				
119B ->122B	0.51913				
Excited State 9:	4.124-A	2.1306 eV	581.92 nm	*f*=0.0000	<S**2>=4.001
120A ->124A	-0.48365				
121A ->125A	-0.48393				

(Continued)

118B ->122B	0.48483				
119B ->123B	0.49031				
Excited State 10:	3.754-A	2.4205 eV	512.22 nm	*f*=0.0000	<S**2>=3.273
122A ->124A	-0.10805				
120B ->122B	0.66576				
121B ->123B	0.72566				
Excited State 11:	4.025-A	2.4288 eV	510.48 nm	*f*=0.0004	<S**2>=3.801
122A ->125A	-0.31288				
123A ->124A	0.31872				
120B ->123B	0.67856				
121B ->122B	0.57159				
Excited State 12:	3.453-A	2.4303 eV	510.17 nm	*f*=0.0000	<S**2>=2.731
122A ->124A	-0.66228				
123A ->125A	0.73272				
121B ->123B	-0.11868				
Excited State 13:	3.132-A	2.4379 eV	508.56 nm	*f*=0.0022	<S**2>=2.203
122A ->125A	0.69667				
123A ->124A	-0.55626				
120B ->123B	0.37148				
121B ->122B	0.25435				
Excited State 14:	3.004-A	2.5075 eV	494.45 nm	*f*=0.0000	<S**2>=2.006
103B ->124B	-0.29206				
103B ->126B	0.10040				
104B ->124B	-0.51360				
104B ->125B	-0.12423				
104B ->126B	0.17568				
110B ->124B	-0.23787				
113B ->124B	0.18928				
115B ->124B	0.58015				
115B ->125B	0.13683				
115B ->126B	-0.18865				
116B ->124B	-0.21328				

(Continued)

Excited State 15:	3.005-A	2.6832 eV	462.07 nm	*f*=0.0000	<S**2>=2.008
99B ->125B	0.12855				
105B ->124B	-0.22981				
105B ->125B	0.45891				
108B ->124B	-0.11181				
111B ->124B	-0.28474				
111B ->125B	0.64954				
119B ->125B	0.11436				
121B ->124B	-0.17104				
121B ->125B	0.32223				
Excited State 16:	4.067-A	2.8990 eV	427.68 nm	*f*=0.0000	<S**2>=3.885
115A ->125A	0.10810				
116A ->124A	-0.22632				
117A ->124A	-0.20772				
118A ->125A	0.47758				
119A ->124A	0.50593				
114B ->123B	-0.12840				
115B ->122B	0.12327				
116B ->122B	0.40538				
117B ->123B	-0.38166				
Excited State 17:	4.076-A	2.9032 eV	427.06 nm	*f*=0.0000	<S**2>=3.903
115A ->124A	0.11568				
116A ->125A	-0.21514				
117A ->125A	-0.19486				
118A ->124A	0.51028				
119A ->125A	0.45750				
114B ->122B	-0.13969				
115B ->123B	0.11344				
116B ->123B	0.38373				
117B ->122B	-0.42289				
Excited State 18:	3.014-A	3.0171 eV	410.94 nm	*f*=0.0000	<S**2>=2.021
101B ->125B	-0.21719				
105B ->125B	-0.11886				
108B ->124B	-0.23911				

(Continued)

108B ->125B	-0.80227				
108B ->126B	0.20541				
111B ->124B	0.14472				
111B ->125B	0.13046				
119B ->125B	-0.26261				
Excited State 19:	3.993-A	3.1922 eV	388.40 nm	*f*=0.0001	<S**2>=3.736
114A ->125A	-0.33682				
115A ->125A	-0.26088				
117A ->124A	0.51344				
118A ->125A	0.11223				
119A ->124A	0.38023				
112B ->123B	0.22620				
114B ->123B	0.32212				
115B ->122B	-0.42032				
Excited State 20:	4.031-A	3.2044 eV	386.92 nm	*f*=0.0000	<S**2>=3.812
114A ->124A	-0.35829				
115A ->124A	-0.28644				
117A ->125A	0.49084				
118A ->124A	0.11402				
119A ->125A	0.32339				
112B ->122B	0.24954				
114B ->122B	0.35652				
115B ->123B	-0.40328				
Excited State 21:	3.165-A	3.2755 eV	378.52 nm	*f*=0.0011	<S**2>=2.255
115A ->125A	-0.11940				
117A ->124A	0.25240				
118A ->125A	-0.26702				
119A ->124A	-0.46767				
116B ->122B	0.54867				
117B ->123B	-0.52503				
Excited State 22:	3.099-A	3.2851 eV	377.41 nm	*f*=0.0000	<S**2>=2.151
115A ->124A	0.10612				
117A ->125A	-0.19500				

(Continued)

118A ->124A	0.35130				
119A ->125A	0.45278				
116B ->123B	-0.49096				
117B ->122B	0.57497				
Excited State 23:	3.105-A	3.5300 eV	351.23 nm	*f*=0.0383	<S**2>=2.160
113A ->124A	-0.13040				
114A ->125A	-0.23478				
115A ->125A	-0.15717				
116A ->124A	0.30679				
117A ->124A	0.34424				
118A ->125A	-0.19251				
119A ->124A	0.29329				
121A ->124A	0.22168				
112B ->123B	-0.21161				
114B ->123B	-0.34793				
115B ->122B	0.49410				
119B ->122B	0.26363				
Excited State 24:	3.083-A	3.5533 eV	348.93 nm	*f*=0.0000	<S**2>=2.126
114A ->124A	-0.29141				
115A ->124A	-0.21193				
116A ->125A	0.24330				
117A ->125A	0.37379				
118A ->124A	-0.15016				
119A ->125A	0.32189				
112B ->122B	-0.25983				
114B ->122B	-0.42496				
115B ->123B	0.47747				
119B ->123B	0.11619				
Excited State 25:	3.397-A	3.5559 eV	348.67 nm	*f*=0.0137	<S**2>=2.634
108A ->125A	0.24817				
113A ->124A	-0.36990				
115A ->125A	0.14837				
116A ->124A	0.52394				
117A ->124A	-0.33723				

(Continued)

118A ->125A	-0.30384				
119A ->124A	0.29292				
112B ->123B	0.14151				
114B ->123B	0.11009				
115B ->122B	-0.21697				
116B ->122B	0.14210				
117B ->123B	-0.16670				
119B ->122B	-0.18362				
Excited State 26:	3.442-A	3.5865 eV	345.69 nm	*f*=0.0000	<S**2>=2.712
108A ->124A	0.27331				
113A ->125A	-0.36149				
115A ->124A	0.18189				
116A ->125A	0.50286				
117A ->125A	-0.33298				
118A ->124A	-0.31580				
119A ->125A	0.36853				
112B ->122B	0.15803				
114B ->122B	0.11546				
115B ->123B	-0.17662				
117B ->122B	-0.16173				
Excited State 27:	3.046-A	3.6156 eV	342.92 nm	*f*=0.2887	<S**2>=2.069
117A ->124A	-0.18786				
120A ->125A	0.10944				
121A ->124A	0.56099				
112B ->123B	0.11988				
114B ->123B	0.17061				
115B ->122B	-0.23517				
119B ->122B	0.68467				
Excited State 28:	3.695-A	3.6977 eV	335.30 nm	*f*=0.0000	<S**2>=3.163
118B ->122B	0.73128				
119B ->123B	-0.66062				
Excited State 29:	4.094-A	3.7179 eV	333.48 nm	*f*=0.0075	<S**2>=3.939
120A ->125A	-0.50223				

(Continued)

121A ->124A	0.57917				
118B ->123B	0.52277				
119B ->122B	-0.35424				
Excited State 30:	3.486-A	3.7196 eV	333.33 nm	*f*=0.0000	<S**2>=2.788
120A ->124A	0.81814				
121A ->125A	-0.51585				
118B ->122B	0.19325				
119B ->123B	0.10269				
Excited State 31:	3.039-A	3.7705 eV	328.82 nm	*f*=0.0000	<S**2>=2.059
120A ->124A	0.23651				
121A ->125A	0.66412				
123A ->131A	0.10539				
118B ->122B	0.39247				
119B ->123B	0.50479				
120B ->132B	0.10515				
121B ->131B	-0.10912				
Excited State 32:	3.003-A	3.7941 eV	326.78 nm	*f*=0.1594	<S**2>=2.004
120A ->125A	0.69566				
118B ->123B	0.69232				
Excited State 33:	3.669-A	4.0448 eV	306.52 nm	*f*=0.0000	<S**2>=3.115
119A ->125A	0.11114				
103B ->123B	-0.10609				
106B ->122B	0.15137				
112B ->122B	-0.58688				
113B ->123B	0.59263				
114B ->122B	0.45551				
Excited State 34:	3.683-A	4.0478 eV	306.30 nm	*f*=0.0000	<S**2>=3.142
103B ->122B	-0.10942				
106B ->123B	0.13457				
112B ->123B	-0.48160				
113B ->122B	0.71769				
114B ->123B	0.40488				

(Continued)

Excited State	35:	3.060-A	4.0849 eV	303.52 nm	*f*=0.0006	<S**2>=2.091
120B ->124B		0.99152				

References.

S1 S. Cueto, H. P. Straumann, P. Rys, W. Petter, V. Gramlich and F. S. Rys, *Acta Cryst. C*, 1992, **48**, 458–460.

S2 S. Kawata, S. Kitagawa, M. Kondo, I Furuchi and M. Munakata, *Angew. Chem., Int. Ed.*, 1994, **33**, 1759–1761.

S3 S. Tanaka, A. Himegi, T. Ohishi, A. Fuyuhiro and S. Kawata, *Acta Cryst. E*, 2014, **70**, m90–m91.

S4 (a) R. Bougon, P. Charpin, K. O. Christe, J. Isabey, M. Lance, M. Nierlich, J. Vigner and W. W. Wilson, *Inorg. Chem.*, 1988, **27**, 1389–1393; (b) T. T. Bangboye, *Inorg. Chim. Acta*, 1988, **151**, 291–295; (c) P. Gerschel, B. Battistella, D. Siegmund, K. Ray and U.-P. Apfel, *Organometallics*, 2020, **39**, 1497–1510.

S5 K. Molčanov and B. Kojić-Prodić, *CrystEngComm*, 2010, **12**, 925–939.